Damping of slow MHD coronal loop oscillations by shocks

E. Verwichte, M. Haynes, T.D. Arber and C.S. Brady

Centre for Fusion, Space and Astrophysics, Department of Physics, University of Warwick, Coventry CV4 7AL, UK

Erwin.Verwichte@warwick.ac.uk

ABSTRACT

The damping of slow magnetoacoustic coronal loop oscillations by shock dissipation is investigated. Observations of large amplitude slow mode observations by SUMER show a clear dependency of the damping rate on the oscillation amplitude. Fully nonlinear MHD simulations of slow mode oscillations in the presence of thermal conduction are performed that show that shock dissipation is an important damping mechanism at large amplitudes, which enhances the damping rate by up to 50% above the rate given by thermal conduction alone. A comparison between the numerical simulations and the SUMER observations shows that, although the shock dissipation model can indeed produce an enhanced damping rate that is function of the oscillation amplitude, the found dependency is not as strong as that for the observations, even after considering observational corrections and the inclusion of enhanced linear dissipation.

Subject headings: plasmas — Sun:corona — Sun:oscillations — waves

1. Introduction

Magnetohydrodynamic (MHD) waves are ubiquitous in the solar corona as demonstrated by the numerous observations of waves in various quite and active coronal structures collected during the past decade (e.g. DeForest & Gurman 1998; Aschwanden et al. 1999; Nakariakov et al. 1999; Verwichte et al. 2005; Foullon et al. 2005), and recently with new instruments (Tomczyk et al. 2007; Okamoto et al. 2007; Doschek et al. 2007). The signatures of coronal MHD waves reveal otherwise hidden physical processes acting in the corona. As such they can be used to constrain theoretical models and to indirectly measure coronal quantities such as the local magnetic field strength through the application of the technique of MHD coronal seismology (for a review see e.g. Nakariakov & Verwichte 2005).

In particular, slow magnetoacoustic waves have been observed as upwardly propagating wave trains in coronal plumes and loops in polarimeter, imaging and spectral data, (e.g. Berghmans & Clette 1999; DeMoortel et al. 2000) and as standing waves (oscillations) in hot coronal loops in spectral data from the Solar Ultraviolet Measurements of Emitted Radiation (SUMER) instrument on SoHO (Kliem et al. 2002; Wang et al. 2002) and the Bragg Crystal Spectrometer (BCS) on Yohkoh (Mariska 2005).

In spectral data the slow mode oscillations were detected as line-of-sight velocity variations. Slow mode osillations are accompanied by intensity variations that are a quarter out of phase in time with respect to the velocity variations (Wang et al. 2003a). However, intensity variations have been observed in only a few of the reported cases. This may be explained in two ways. Firstly, the fundamental slow mode has a density perturbation that is anti-symmetric with respect to the loop top. This implies for BCS, which is a full-disk imager, that the total density variation integrated along the entire loop is equal to zero. Finite density variations can only be detected if the loop is partially occulted by the limb. Furthermore, at the loop location where the velocity perturbation is the largest, the density perturbation of the mode has a node and is small. Therefore, for SUMER, which measures along a one-dimensional slit that crosses the oscillating loop, measuring simultaneously a significant velocity and intensity variation is not guaranteed. Secondly, some of the reported oscillations when only observed as velocity variations, may not be slow but fast magnetoacoustic kink modes instead, especially when the oscillation characteristics resemble those of transverse loop oscillations observed by TRACE.

These waves have periods of about 2-7 mins and relative density amplitudes of typically less than 5 %. SUMER oscillations, observed mainly in a bandpass sensitive to 6.3 MK hot plasma, have periods and decay times in the ranges of 7-30 and 6-37 mins, respectively (Wang et al. 2003b). Various physical damping mechanisms have been investigated (see Nakariakov & Verwichte 2005,and references therein) and thermal conduction has been found to have the strongest effect. However, when the wave amplitude is large nonlinear effects may also be important. Although the observed slow propagating wave trains and BCS oscillations have velocity amplitudes typically less than 5% sonic Mach and can therefore be considered linear, SUMER oscillations have much larger velocity amplitudes up to 70% Mach. Figure 1 shows the observed damping times as a function of the periods. The SUMER data set has been split into two subsets: 30 events for which the Mach number is less or equal to 0.2 and 24 events for which it is larger than 0.2. The damping times of both subsets scale approximately linearly with the period (Ofman & Wang 2002). However, the large amplitude subset has a damping time 1.5-2.0 times shorter than the small amplitude subset. There is a tendency for larger amplitude oscillations to have shorter damping times. This is a clear indication that nonlinear effects are influencing the damping rate of the SUMER oscillations. One of

the possible nonlinear mechanisms is shock formation and dissipation. Indeed, Haynes et al. (2008) showed numerically that in the absence of thermal conduction, large amplitude slow mode oscillations still damp rapidly due to shock dissipation. This paper investigates for the first time the role of shock dissipation in the damping of slow mode oscillations in coronal loops, in the presence of thermal conduction.

This paper is structured as follows. In Sect. 2 the basic theory of the shock dissipation mechanism for one-dimensional acoustics is briefly introduced. In Sect. 3 the numerical simulations of nonlinear slow mode oscillations in the presence of thermal conduction are presented. In Sect. 4, the theoretical results are compared with the observed characteristics of SUMER oscillations. Finally, in Sect. 5 the main findings are discussed.

2. Dissipation model

Long wavelength slow magnetoacoustic oscillations in uniform coronal loops are basically longitudinal modes with little dispersion, and for typical coronal conditions have a phase speed less than 10% below the sound speed $C_{\rm s}$. Therefore, the slow mode can be modelled as two counter-propagating one-dimensional sound waves along the magnetic field with frequency ω and wave number k. The effects of dissipation by thermal conduction and shocks are initially discussed separately. The combined effect of the two dissipation mechanisms is treated numerically and discussed later.

In the solar corona, parallel electron thermal conduction and to a lesser extend viscosity and resistivity, are important dissipative processes for slow mode oscillations (e.g. DeMoortel & Hood 2003). The dispersion relation for sound waves that includes linear thermal conduction is a cubic equation in ω, i.e.

$$\omega^3 + {\rm i}\eta C_{\rm s} k \omega^2 - C_{\rm s}^2 k^2 \omega - {\rm i}\eta C_{\rm s}^3 k^3/\gamma \; = \; 0 \; , \tag{1}$$

where $\eta = \gamma(\gamma-1)Tk\kappa_{\parallel}/\rho C_{\rm s}^3$ with $\kappa_{\parallel}$ the Braginskii parallel electron thermal conduction, which is given as $\kappa_{\parallel} = \kappa_{\rm o} T^{5/2}$ Wm^{-1}K^{-1}. The parameter $\kappa_{\rm o} = 10^{-11}$ is a function of fundamental constants, the ion charge state (taken to be unity) and the Coulomb logarithm (a weak function of density and temperature, assumed constant) (Braginskii 1965). The damping rate is given by the imaginary part of the relevant root. For a typical coronal loop of length $L = 200$ Mm, density $\rho = 10^{-12}$ kgm^{-3} and temperature $T = 1.0$ MK, $\eta = 0.05 \ll 1$. In that case, thermal conduction only weakly affects the wave solution and an approximate solution may be used, i.e. $\tau_{\rm lin} \approx 2\rho C_{\rm s}^2/(\gamma-1)^2 T k^2 \kappa_{\parallel}$. However, for the same coronal loop at a temperature of 6 MK, $\eta = 1.6$ and the full cubic equation has to be solved. This means that the thermal conduction damping time $\tau_{\rm lin}$ of SUMER oscillations is of the same order

as the oscillation period $P_{\rm lin}$ and that the period itself is substantially modified by thermal conduction.

It is well-known that in the limit of zero dissipation large amplitude sound waves form shocks. The relevant results are briefly repeated here (see also sections 101 and 102 of Landau & Lifshitz 1959). The velocity of a polytropic simple sound wave is described by the functional

$$V \;=\; F\left[x - \left(\pm C_{\rm s} + \frac{1}{2}(\gamma+1)V\right)t\right] \;, \tag{2}$$

where $C_{\rm s}$ is the speed of sound and γ is the the ratio of specific heats, taken to be 5/3. The functional $V(t{=}0) = F(x)$ describes the original shape of the wave. Here, $F(x) = V_0\,\sin(kx)$ where $k = n\pi/L$ with n the harmonic wave number and L the loop length. A discontinuity will have formed when $\partial V/\partial x$ becomes infinite locally for the first time. This occurs when

$$t_{\rm sf} \;=\; \frac{P}{(\gamma+1)\,\pi M_0} \;, \tag{3}$$

with P the wave period and $M_0 = V_0/C_{\rm s}$ the wave amplitude Mach number. Once a shock is formed, the wave shape will resemble a sawtooth. The part of the wave in front (behind) of the shock moves slower (faster) than the shock and will advect into (be caught by) the shock. At the shock wave energy is converted into thermal energy. During this process the wavelength remains the same. This leads to the temporal evolution of the velocity amplitude, taking into account the shock formation time, as

$$V(t) \;=\; \frac{V_0}{1 + H(t-t_{\rm sf})(t-t_{\rm sf})/\tau_{\rm sd}} \;, \tag{4}$$

with

$$\tau_{\rm sd} \;=\; \frac{P}{(\gamma+1)\,M_0} \;, \tag{5}$$

and where H(x) is the Heaviside function.

What is the effect of combining thermal conduction and shock dissipation? Weakly dissipative and nonlinear effects for a sound wave naturally leads to the study of the nonlinear Burgers equation (Whitham 1927), which supports shocks in the limit of vanishing dissipation. Including the effects of gravitational stratification (Nakariakov et al. 2000) or variations in loop cross-section (Verwichte et al. 2001) leads to a modified Burgers equation with an additional geometrical term. However, because the role of thermal conduction cannot be considered weak, we prefer to model the wave behaviour numerically.

3. Numerical simulations

Numerical simulations of slow magnetoacoustic oscillations were performed using the code Lare (Arber et al. 2001) which numerically integrates the fully nonlinear non-ideal MHD equations in normalised, Lagrangian form. Braginskii parallel electron thermal conduction as defined earlier has been included. Due to the severe numerical stability constraint imposed by diffusive terms, i.e. time step must vary as cell size squared, the thermal conduction term in the energy equation is treated implicitly. The advective/compressive terms are handled explicitly as described in Arber et al. (2001). Reflecting boundary conditions have been used with zero thermal flux through the boundaries. The numerical simulations have been performed with 128 grid points. Selected simulations with a larger resolution of 1024 grid points have been performed to verify convergence. The temporal evolution of a slow magnetoacoustic oscillation in one dimension is studied on a uniform loop of length 200 Mm, density 10^{-12} kgm^{-3} and temperature 6.3 MK. Initially the velocity perturbation of a fundamental slow mode is set up, i.e. $V(x) = M_0\, C_{\rm s}\, \sin(\pi x/L)$.

First, simulations have been performed without thermal conduction to show the shock dissipation mechanism by setting $\kappa_{\rm o} = 0$. Figure 2 shows the temporal evolution of the mode velocity at the loop top for various velocity amplitudes. The damping is solely governed by shock dissipation. The oscillation envelope follows Eq. (4), which is shown as dotted lines in the figure. The small discrepancies between the analytical oscillation envelope and the numerical oscillation profile are due to the details of the shocked standing wave profile. For comparison, the velocity profile for a small (linear) amplitude oscillation with thermal conduction is overplotted. It can be seen that for Mach numberd above approximately 0.5, shock dissipation damps the oscillation at least as strongly as thermal conduction. However, the presence of thermal conduction will influence the shock dissipation rate.

Shock dissipation will still occur in the presence of thermal conduction. Instead of an infinitely thin shock, a finite-sized dissipation region is formed into which the wave field is advected and converted into thermal energy. Before the shock structure is formed, thermal conduction is the only dissipation mechanism. Hence, the wave amplitude decreases initially exponentially. Nonlinearity will still steepen the velocity profile into a shock, but because the time for the shock to form is a function of wave amplitude, this is delayed in comparison with the case without thermal conduction. The amount of delay itself will be a function of the initial wave amplitude.

The results of the numerical simulation with thermal conduction (setting $\kappa_{\rm o} = 10^{-11}$) are as follows. Figure 3 shows that the velocity profile along the loop steepens nonlinearly to form a shock. The shock is non-stationary, bouncing back and forth in the loop. This is because the shock is the superposition of the shocks of the two counter-propagating slow waves.

Figure 4 shows the temporal evolution of the mode velocity at the loop top for various velocity amplitudes with thermal conduction included. Especially for larger velocity amplitudes, it is clear from comparing velocity profile for a small (linear) amplitude oscillation with thermal conduction, that the damping rate of the mode exceeds that from linear theory.

Figure 5 shows the inverse quality factor P/τ as a function of Mach number. The period and damping times are calculated from a fit of an exponentially decaying cosine to the numerical time profile at a fixed spatial location. At small Mach number, the quality factor tends as expected to the linear damping due to thermal conduction. The inverse quality factor grows with the Mach number up to 50% above the linear case. Also, for large Mach numbers, nonlinearity is the strongest damping mechanism. This can be seen by the decreasing difference between P/τ for the cases with and without thermal conduction. Also, the combined effect of nonlinearity and thermal conduction is less than the superposition of the two separate damping rates, by about 30%. One reason for this is the earlier discussed delay of shock formation due to thermal conduction. Finally, the damping rate is a function of location along the loop due to the non-harmonic profile. However, this introduces a difference of less than 10%.

4. Comparison with SUMER observations

Wang et al. (2003b) studied 54 events of slow magnetoacoustic loop oscillations using SUMER. The observed decay time is characterised by an e-folding time τ. Wang et al. (2003b) reported for each event the maximum Doppler velocity and the Doppler velocity amplitude of a fitted damped oscillation. The latter quantity is used here as it better represents the whole oscillation time interval rather than only the start. However, we visually re-inspected the large amplitude events through the plots provides by Wang et al. (2003b), and have concluded that for six events (4C, 11B, 15A, 15C, 19A and 19B) the reported fitted amplitude grosely overestimates the observed oscillation velocity amplitude.

Figure 6 shows the inverse quality factor P/τ as a function of Mach number. If the damping was due to linear processes, then there should be no correlation. The observations shows that the inverse quality factor grows linearly strongly with Mach number with a slope of 2.9 ± 0.3. However, because the oscillations are not necessarily measured at the loop tops where the oscillation velocity is the largest, the measured Mach number may be underestimated. Therefore, the observational slope can be smaller in reality. We estimate by how much the the slope could be reduced as follows. With uniform sampling of loop locations, the average measured velocity amplitude for a linear oscillation is $M_0 C_s < \sin(\pi x/L) > = M_0 C_s 2/\pi$. The loop top velocity amplitude is then estimated to be on average by a factor $\pi/2$ larger

than the measured amplitude. This factor is strictly speaking only valid for a pure harmonic oscillation where the standing velocity profile does not change with position. However, it remains a reasonable approximation for the first stage of the nonlinear oscillations, when the shock structure has not yet formed. Hence, this effect may account for the slope of the fit to be lowered at most to a value of 1.8 ± 0.2.

The horizontal dashed line presents the inverse quality factor $P_{\rm lin}/\tau_{\rm lin}$ for a fundamental slow mode oscillation in a coronal loop with length, density and temperature as used in the above described numerical simulations. For a realistic range of loop lengths and densities, with the temperature fixed at 6.3 MK gives an inverse quality factors ranging between 0.5 and 0.9. The observed values of P/τ at low Mach numbers fall in that range. However, the addition of the effects of viscosity, radiative losses and gravitational stratification may increase the inverse quality factor by approximately another 20% (Mendoza-Briceno et al. 2004; Bradshaw & Erdélyi 2008). From this we confirm that thermal conduction is the main damping mechanism for small amplitude coronal slow magnetoacoustic waves.

The effect of shock dissipation is to make the inverse quality factor grow with Mach number above the level of linear dissipation. Figure 6 shows that the inverse quality factor from the numerical simulations underestimates the observational result. The disparity is not as large if taking into account the above discussed reduced observational slope and enhanced linear dissipation. However, there is still a clear difference between the observations and the theoretical model. The numerical simulations have also been repeated for coronal loops of 100 Mm length or 8 MK temperature. The linear dissipation rate was found to be lower ($P_{\rm lin}/\tau_{\rm lin} \approx 0.5$)), but the nonlinear behaviour was found to be similar.

5. Conclusions

The SUMER observations independently indicate that nonlinear effects are strongly influencing the damping of large amplitude slow magnetacoustic loop oscillations (see e.g. Fig. 1). Therefore, for large amplitude slow mode oscillations, linear processes such as thermal conduction are not sufficient to explain the observations. We have investigated the effect of shock formation and dissipation in a one-dimensional model of a slow mode oscillation is a homogeneous loop in the presence of thermal conduction. Because at the large temperature sampled by SUMER the effect of thermal conduction on the mode behaviour cannot be considered weak, a fully nonlinear numerical approach has been favoured above an analytical approach. The numerical simulations can indeed produce an enhanced damping rate that is function of the oscillation amplitude, and which is up to 50% larger than given by thermal conduction alone. However, the found dependency is not as strong as that

for the observations, even after considering corrections for observational sampling and the inclusion of enhanced linear dissipation and gravitational stratification. Also, contrary to the simulations, the SUMER observations show smooth velocity time profiles without major discontinuities. This may be due to the neglect in the modelling of the effect of transverse loop structuring on the shock structure, and its subsequent observational signature.

The investigation of nonlinear slow magnetoacoustic oscillations in coronal loops may be extended to explicitely include effects such as viscosity, gravitational stratification (Nakariakov et al. 2000), radiative losses (Nakariakov et al. 2004; Bradshaw & Erdélyi 2008), loop cross-section (Verwichte et al. 2001; DeMoortel & Hood 2004), transverse structuring (Voitenko et al. 2005), excitation (Nakariakov et al. 2004) and curvature (Verwichte et al. 2006). Furthermore, more observational examples of large amplitude slow mode oscillations are required to confirm their true identity and the trend observed by SUMER, using for example the EUV imaging spectrometer and X-ray/EUV telescope on Hinode.

E.V. wishes to acknowledge the financial support from the UK Engineering and Physical Sciences Research Council. Furthermore, the authors wish to acknowledge the anonymous referee for the valuable comments.

REFERENCES

Arber, T.D., Longbottom, A. W., Gerrard, C. L., & Milne, A. M. 2001, J. Comput. Phys., 171, 151

Aschwanden, M.J., Fletcher, L., Schrijver, C.J. & Alexander, D., 1999, ApJ, 520, 880

Berghmans, D. & Clette, F., 1999, Sol. Phys., 186, 207

Bradshaw, S.J. & Erdélyi, R., 2008, A&A, in press

Braginskii, S.I., 1965, Rev. Plasma Phys., 1, 205

DeForest, C. E. & Gurman, J. B., 1998, ApJ, 501, L217

De Moortel, I., Ireland, J. & Walsh, R. W., 2000, A&A, 355, L23

DeMoortel, I. & Hood, A.W., 2003, A&A, 408, 755

DeMoortel, I. & Hood, A.W., 2004, A&A, 415, 705

Doschek, G.A., Mariska, J.T., Warren, H.P., Brown, C.M., Culhane, J.L., Hara, H., Watanabe, T., Young, P.R. & Mason, H.E. 2007, ApJ, 667, L109

Foullon, C., Verwichte, E., Nakariakov, V.M. & Fletcher, L., 2005, A&A, 440, L59

Haynes, M., Arber, T.D. & Verwichte, E.: 2007, A&A, 479, 235

Kliem, B., Dammasch, I. E., Curdt, W. & Wilhelm, K., 2002, ApJ, 568, L61

Landau, L.D. & Liftshitz, E.M., 1959: Fluid Mechanics, Pergamon Press, Oxford, United Kingdom

Mariska, J. T., 2005, ApJ, 620, L67

Mendoza-Briceno, C.A., Erdelyi, R. & Sigalotti, L.D. 2004, ApJ, 605, 493

Nakariakov, V.M., Ofman, L., DeLuca, E.E., Roberts, B. & Davila, J.M., 1999, Science, 285, 862

Nakariakov, V.M., Verwichte, E., Berghmans, D. & Robbrecht, E., 2000, A&A, 362, 1151

Nakariakov, V.M., Tsiklauri, D., Kelly, A., Arber, T.D. & Aschwanden, M.J., 2004, A&A, 414, L25

Nakariakov, V.M. & Verwichte, E. 2005, Living Rev. Solar Phys. 2, (2005), 3. URL (cited on 2005-07-05): http://www.livingreviews.org/lrsp-2005-3

Ofman, L. & Wang, T. J., 2002, ApJ, 580, L85

Okamoto, T.J., Tsuneta, S., Berger, T.E., Ichimoto, K., Katsukawa, Y., Lites, B.W., Nagata, S., Shibata, K., Shimizu, T., Shine. R.A., Suematsu, Y., Tarbell, T.D. & Title, A.M., 2007, Science, 318, 157 Nakariakov, V. M., 2001, A&A, 370, 591

Tomczyk, S., McIntosh, S.W., Keil, S.L., Judge, P.G., Schad, T., Seeley. D.H. & Edmondson, J., 2007, Science, 317, 1192

Voitenko, Y., Andries, J., Copil, P.D. & Goossens, M., 2005, A&A, 437, L47

Wang, T. J., Solanki, S. K., Curdt, W., Innes, D. E. & Dammasch, I. E., 2002, ApJ, 574, L101

Wang, T.J., Solanki, S.K., Innes, D.E., Curdt, W. & Marsch, E., 2003a, A&A, 402, L17

Wang, T. J., Solanki, S. K., Curdt, W., Innes, D. E., Dammasch, I. E. & Kliem, B., 2003b, A&A, 406, 1105

Verwichte, E., Nakariakov, V.M., Berghmans, D. & Hochedez, J.-F., 2001, ESA SP, 493, 395

Verwichte, E., Nakariakov, V.M. & Cooper, F.C., 2005, A&A, 430, L65

Verwichte, E., Foullon, C. & Nakariakov, V.M., 2006, A&A, 446, 1139

Whitham, G.B., 1927: Linear and nonlinear waves, Wiley-interscience, United States.

Zhugzhda, Y.D., 2004, Phys. Plasmas, 11, 2256

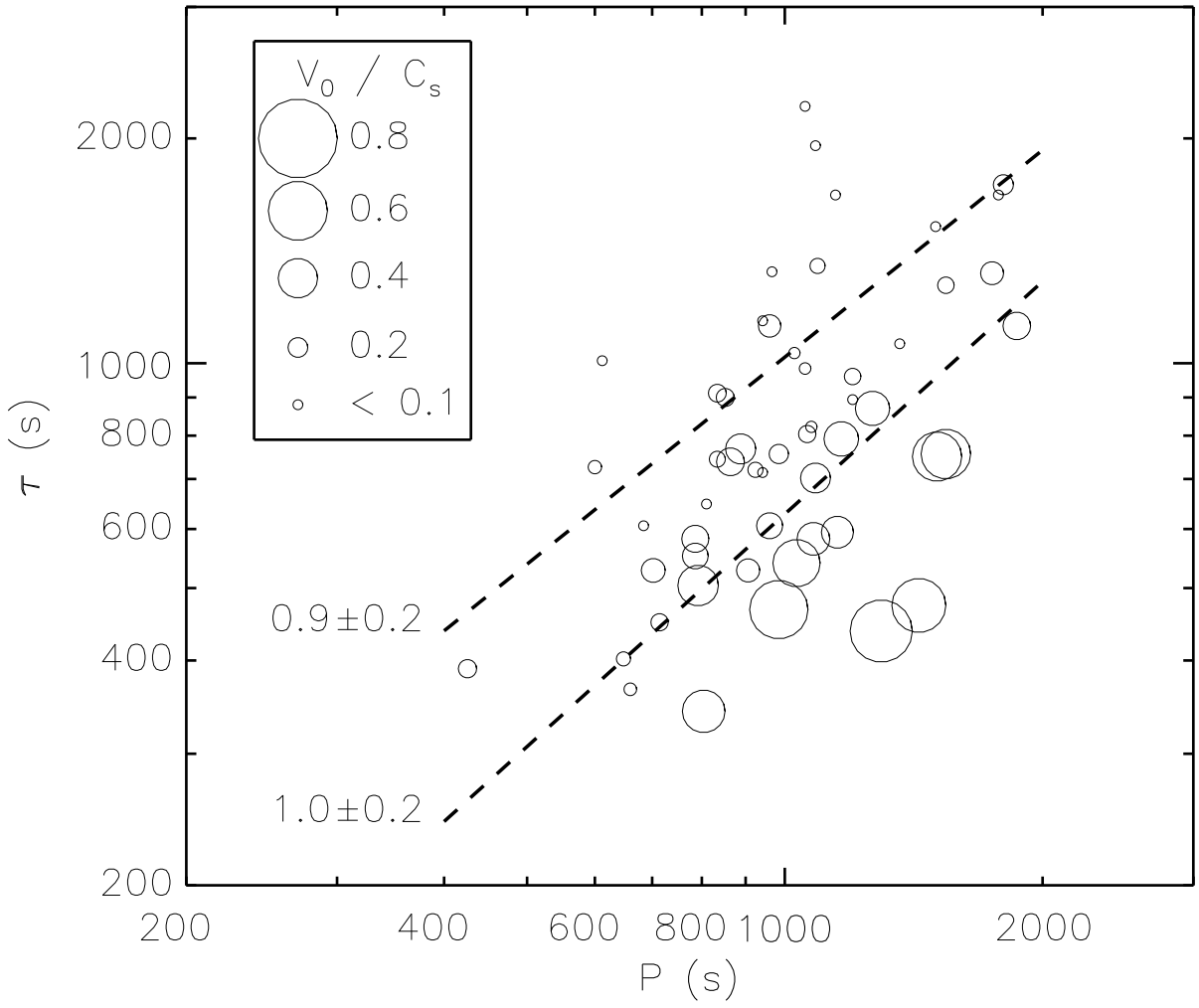

Fig. 1.— Observed damping time versus period of the SUMER events studied by Wang et al. (2003b). The size of the symbol circles is related to the Mach number of the velocity amplitude. The two dashed lines are least-square fits of the events with velocity amplitudes $V_0 \leq 0.2C_s$ (top) and $V_0 > 0.2C_s$ (bottom). The value of the slope is indicated.

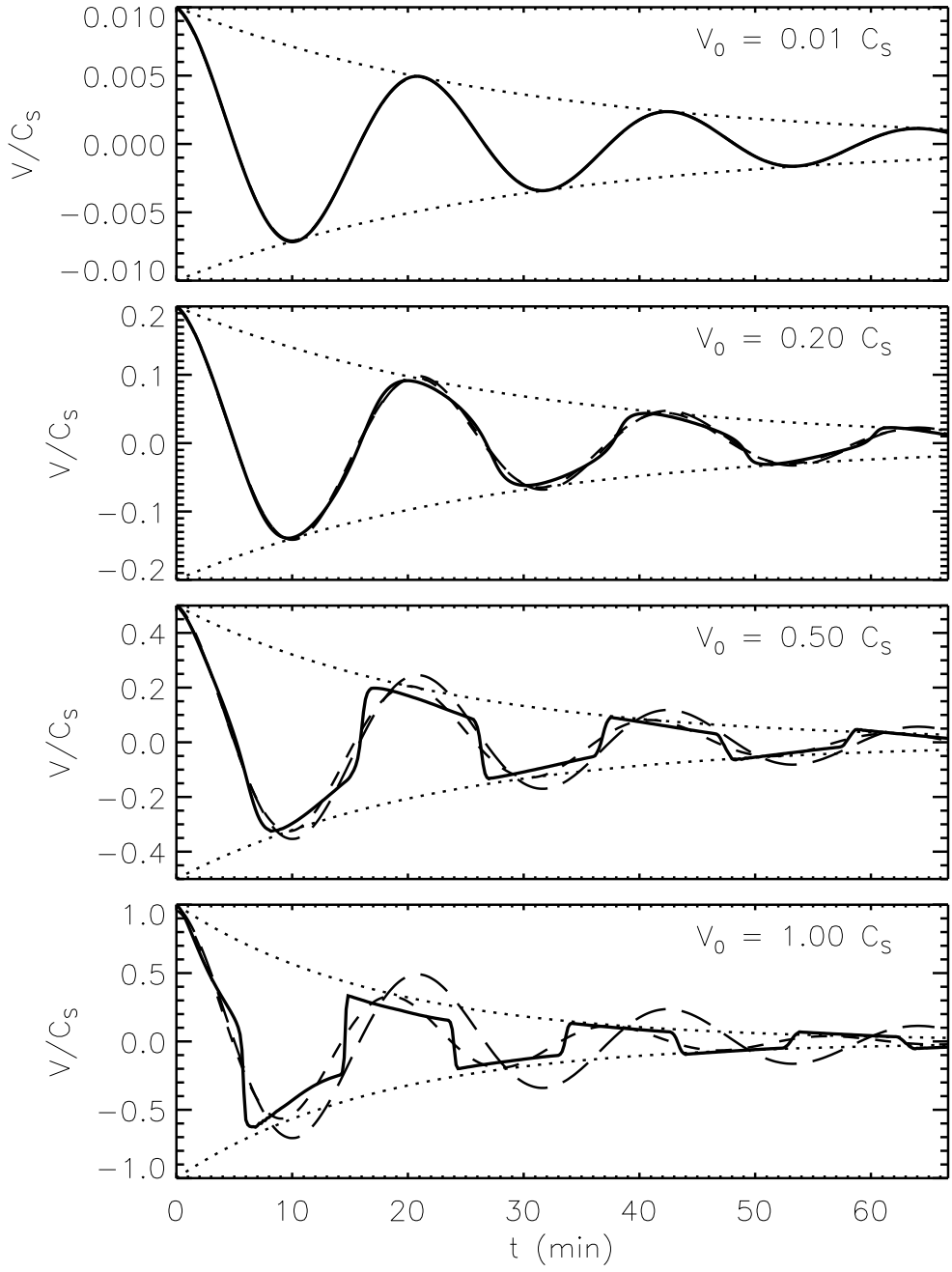

Fig. 2.— Temporal evolution of the velocity at the loop top for four different velocity amplitudes (solid curve) for numerical simulations without thermal conduction. i.e. $\kappa_o = 0$. The dashed curve is a fitted exponentially damped cosine oscillation with its envelope (dotted curves). For comparison, the long-dashed line is the velocity profile for a small amplitude (linear) oscillation that is damped solely by thermal conduction.

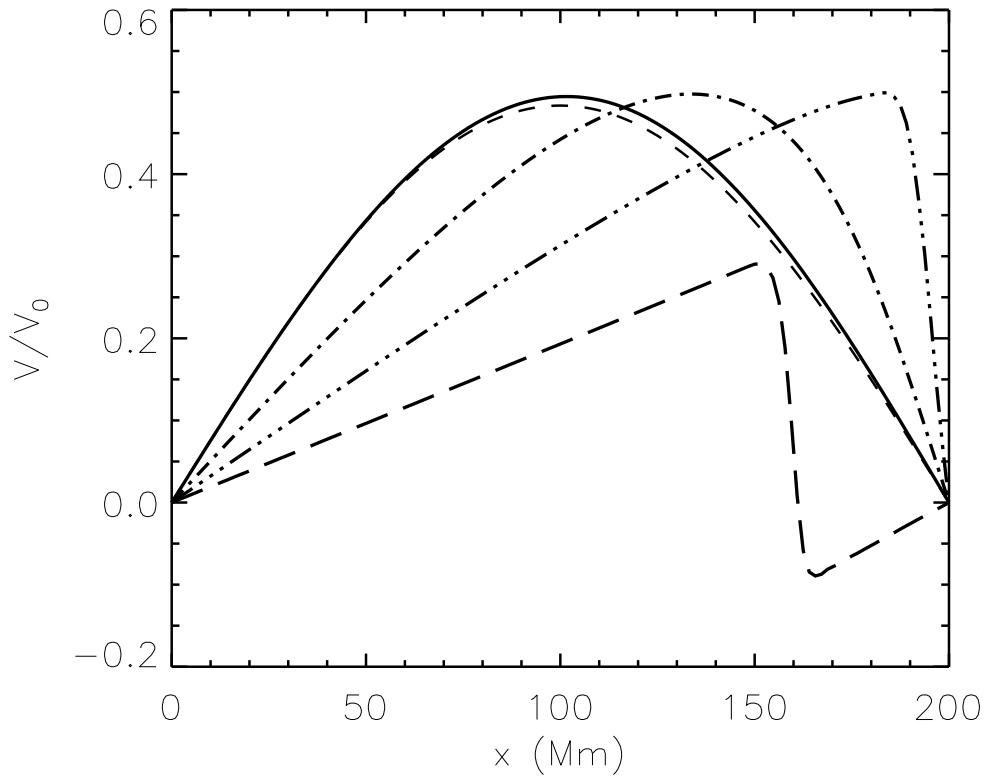

Fig. 3.— Normalised velocity profile, $V(t)/V_0$, of a fundamental mode at time t= 21 min = 0.97 $P_{\rm lin}$ as a function of distance along the loop for four values of M_0: 0.01 (solid), 0.2 (dot-dashed), 0.5 (dotted-dashed) and 1.0 (long-dashed), in the presence of thermal conduction $\kappa_{\rm o} = 10^{-11}$. The dashed line is the normalised velocity profile of a small amplitude (linear) mode which is damped solely by thermal conduction.

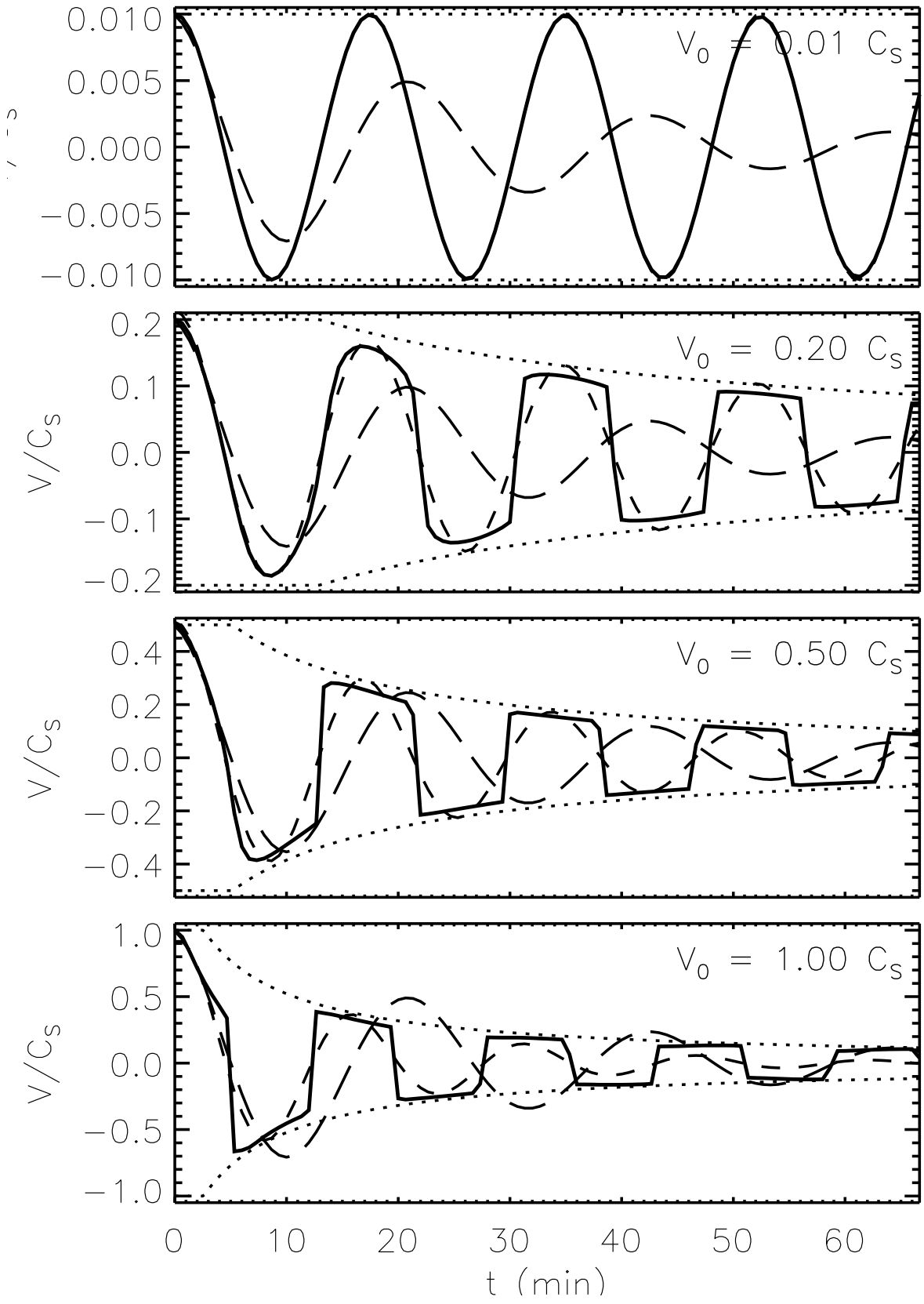

Fig. 4.— Temporal evolution of the velocity at the loop top for four different velocity amplitudes (solid curve), in the presence of thermal conduction $\kappa_o = 10^{-11}$. The dashed curve is a fitted exponentially damped cosine oscillation with its envelope (dotted curves). For comparison, the long-dashed line is the velocity profile for a small amplitude (linear) oscillation that is damped solely by thermal conduction.

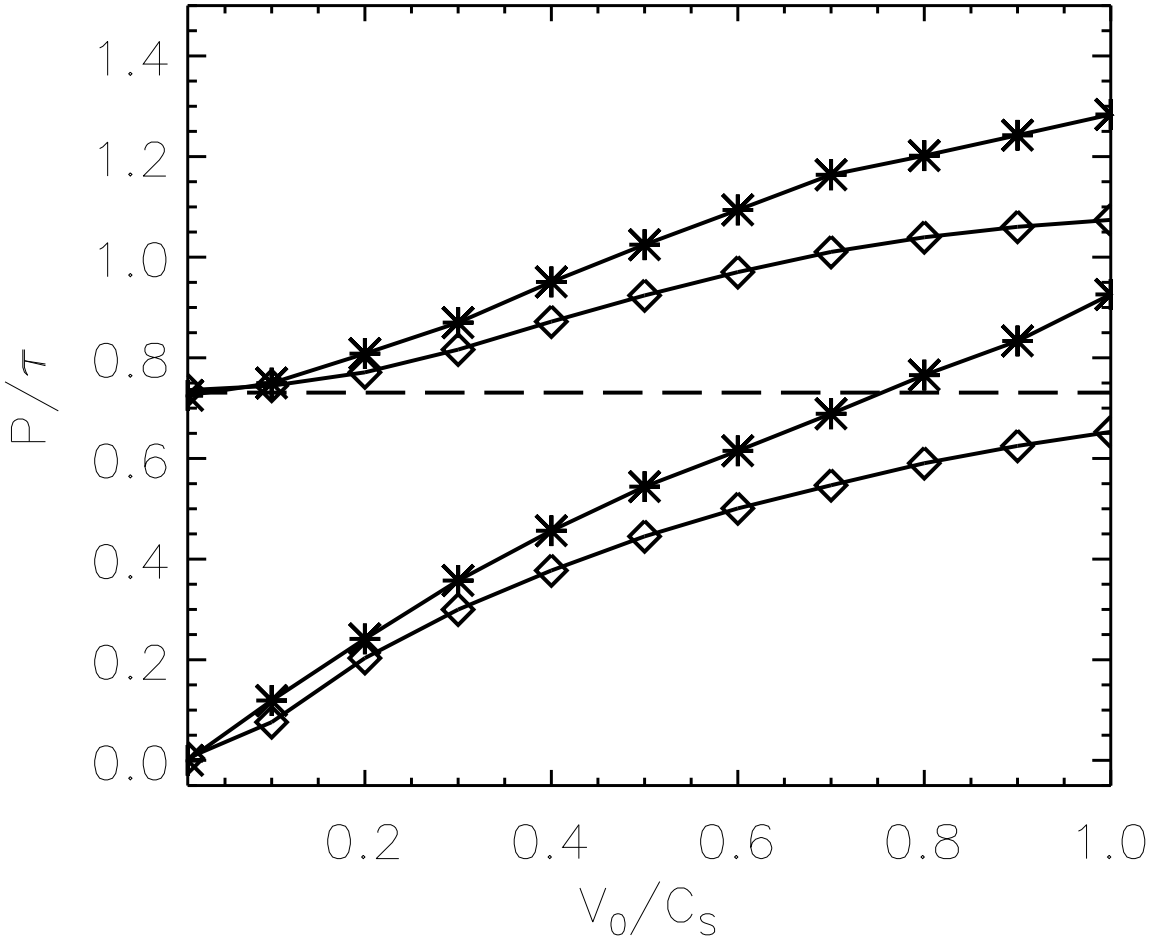

Fig. 5.— Inverse oscillation quality factor P/τ as a function of Mach number M_0 for two sets of numerical simulations. The first set of curves starting at $P/\tau = 0$ for zero Mach number are from the numerical simulations without thermal conduction, i.e. $\kappa_o = 0$. The second set of curves starting at $P_{\rm lin}/\tau_{\rm lin}$ for zero Mach number correspond to numerical simulations with thermal conduction, i.e. $\kappa_o = 10^{-11}$. The curves with diamond symbols represent the inverse quality factor determined from fitting a exponentially decaying cosine at the loop top. The curves with star symbols correspond to the inverse quality factor determined from an exponential fit to the oscillation envelope measured at the loop top. The horizontal dashed line correspond to the value $P_{\rm lin}/\tau_{\rm lin}$.

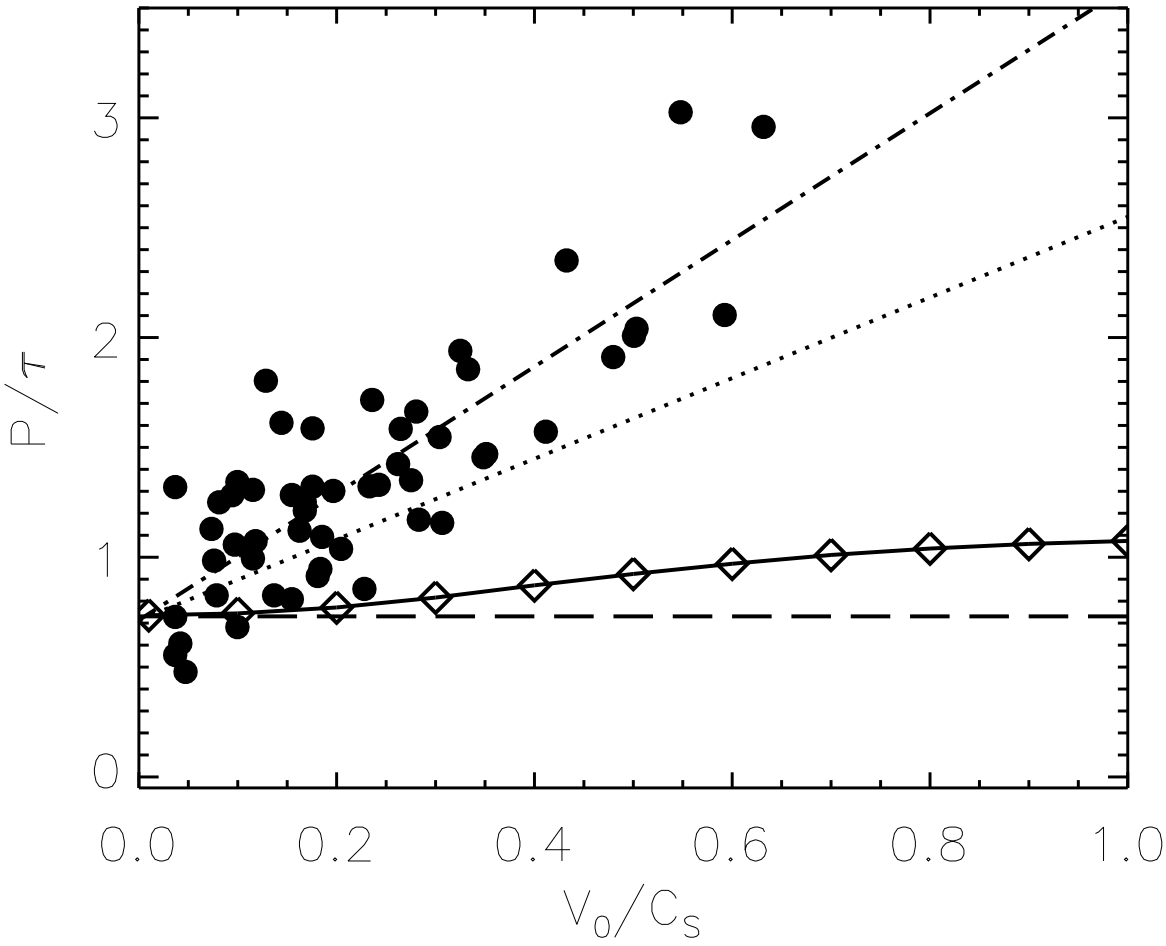

Fig. 6.— Inverse quality factor P/τ as a function of Mach number $M_0 = V_0/C_s$ of the SUMER events (circles). The dot-dashed line is a best linear fit to the data. The dotted line is the fitted line where the slope has been reduced by a factor $2/\pi$. The horizontal dashed line is the inverse quality factor $P_{\rm lin}/\tau_{\rm lin}$ of a small amplitude (linear) oscillation due to thermal conduction. The solid line with diamond symbols is the inverse quality factor determined from fitting to the numerical data at the loop top an exponentially decaying cosine.